

NGC 4993 the shell galaxy host of GW170817: constraints on the recent galactic merger

Ivana Ebrova¹* and Michal Bilek²

¹*Nicolaus Copernicus Astronomical Center, Polish Academy of Sciences, Bartycka 18, 00-716 Warsaw, Poland*

²*Astronomical Institute, Czech Academy of Sciences, Bocnı II 1401/1a, CZ-141 00 Prague, Czech Republic*

Accepted . Received ; in original form

ABSTRACT

NGC 4993 is the shell galaxy host of the GRB170817A short gamma-ray burst and the GW170817 gravitational-wave event produced during a binary neutron star coalescence. The galaxy shows signs, including the stellar shells, that it recently accreted a smaller late-type galaxy. The accreted galaxy could have been the original host of the binary neutron star. We measure the positions of the stellar shells of NGC 4993 in an HST/ACS archival image and use them to constrain the time of the galactic merger. According to the analytical model of the evolution of the shell structure in the expected gravitational potential of NGC 4993, the galactic merger happened at least 200 Myr ago with a probable time roughly around 400 Myr and the estimates and higher than 600 Myr being improbable. Because the galactic merger has likely shut down the star formation in the accreted galaxy, this constitutes the lower limit on the age of the binary neutron star, if it originated in this galaxy.

Key words: gravitational waves – stars: neutron – galaxies: interactions – galaxies: peculiar – galaxies: individual: NGC 4993 – gamma-ray burst: individual: GRB 170817A

1 INTRODUCTION

NGC 4993 galaxy is the host of the optical counterpart (SS17a, Coulter et al. 2017) of the gravitational-wave event GW170817 (Abbott et al. 2017). The gravitational waves were accompanied with a short gamma-ray burst (sGRB), GRB170817A, and followed by the ultraviolet, optical and near-infrared emission. The event is explained as a binary neutron star coalescence.

NGC 4993 is an early-type galaxy. Palmese et al. (2017) argued that the properties they measured, qualify the galaxy as an atypical sGRB host (see their Figure 2). Similarly, Fong et al. (2017) concluded that NGC 4993 is superlative in terms of its large luminosity, old stellar population age, and low star formation rate compared to previous short GRB hosts. On the other hand, Im et al. (2017) found out NGC 4993 to be at the old end of the stellar-age range but similar to some host galaxies of sGRBs. According to Levan et al. (2017), NGC 4993 is consistent with the distributions seen for sGRBs although the offset of the GW170817 source position, with respect to the galactic center and normalized by the effective radius of the galaxy, is closer than about 90 % of short GRBs. All three works agree that there is no or very little ongoing star formation in the galaxy. However, the sit-

uation for NGC 4993 is bit more complex. The galaxy shows several signs that it underwent a relatively recent galactic merger¹, thus the binary neutron star could have come from the secondary galaxy that had different properties. The following evidence suggests that the accreted secondary was a smaller late-type galaxy.

NGC 4993, also known as the shell galaxy MC 1307–231 (Malin & Carter 1983), possesses several stellar shells visible already in Digitized Sky Survey (DSS) images and even more pronounced in recent Hubble Space Telescope (HST) archival data. Shell galaxies account for roughly 10 % of early-type galaxies (e.g., Malin & Carter 1983; Atkinson et al. 2013). Their origin and properties are well explained by a model, where the shells are made of stars from a galaxy accreted on the host on a highly eccentric orbit (e.g., Quinn 1984; Dupraz & Combes 1986; Hernquist & Quinn 1988; Ebrova et al. 2012; Pop et al. 2017).

The HST image also uncovers a rich dust structure around the center of the galaxy. NGC 4993, as a big early-type galaxy, is expected to contain limited amount of gas, thus it is probable that the observed dust lanes could come from the accreted galaxy. Also the possible low-luminosity active galactic nucleus (Palmese et al. 2017; Levan et al.

¹ In this paper, the term ‘merger’ always refers to the merger of galaxies, not to the binary neutron star coalescence

* E-mail: ebrova.ivana@gmail.com

2017; Wu et al. 2017) could have been triggered by gas brought to the central region by the intruding late-type galaxy.

Further evidence that the accreted galaxy was a gaseous late-type galaxy was reported in Palmese et al. (2017). The systematic change of Sersic index and position angle of the fitted light profile for different bands suggests that there could be two stellar populations overlaid with different orientations. Moreover their spectral energy distribution fits prefer younger stellar ages in the outer regions. These regions seem to be associated with the shells.

In the galaxy-merger scenario, shells are formed by the stars currently located near the apocenters of their very eccentric orbits. The shells emerge after the first close pericentric passage of the galaxies and can easily survive several gigayears (e.g., Ebrova et al. 2012; Pop et al. 2017) and possibly even longer than a Hubble time (Dupraz & Combes 1986). Their unique shell kinematics allows connecting the gravitational potential of the galaxy, the merger time (i.e. the time elapsed since the galaxies merged, also referred as the ‘shell-system age’ in this paper), and galactocentric positions of the shell edges (Quinn 1984; Dupraz & Combes 1986; Ebrova et al. 2012; Bilek et al. 2013, 2014).

Here we use publicly available images and data from literature to measure shell positions, construct the gravitational potential and infer the merger time. It would be hard to measure the star-formation history of the secondary galaxy, since the galaxy is now dissolved and overlaid on the body of a more massive galaxy. The merger time can serve as an estimate of the time when the star formation probably stopped due to the disintegration of the accreted galaxy. Our estimate can provide constraints on the models of the evolution of the binary neutron star.

2 SHELLS OF NGC 4993

We adopt the NGC 4993 distance of 41.0 Mpc – the combined redshift and Fundamental-Plane value from Hjorth et al. (2017). The value is consistent with the surface-brightness-fluctuation distance to NGC 4993 derived in Cantiello et al. (2018). One arcsecond corresponds to 0.199 kpc.

We use the publicly available Advanced Camera for Surveys (ACS) F606W Hubble Space Telescope (HST) image of NGC 4993 obtained on April 28, 2017 (exposure time 696 s). The outermost detected shell is near the edge of the HST image. We also examined the publicly available data from Dark Energy Camera (DECam) taken on Jun 04 – Jun 09, 2015 (360 s in r and 100 s in g filters). DECam is installed at 4-meter telescope at the Cerro Tololo Inter-American Observatory (CTIO) in Chile and it has a field of view of roughly 2.2 degree in diameter. We found no additional shells in the DECam image thus all following measurements of the shells are performed on the HST data.

We detected the shells visually in the HST/ACS data. The image of the galaxy is presented in Fig. 1. All shells could be detected either by a linear scaling of the image or after applying the minimum masking technique (see Appendix B in Bilek et al. 2016) with the filter size of 1.2'' (right-hand panel of Fig. 1). The minimum masking improved the visibility of some of the shells, particularly those

Table 1. Measured shell-edge radii of NGC 4993

Shell radius	Detection method
-12.2''	minimum masking
13.75''	minimum masking
17.9''	linear scaling
-18.1''	linear scaling
-25.2''	linear scaling
26.55''	linear scaling
-35.25''	linear scaling
40.65''	linear scaling
-54.55''	linear scaling
65.85''	linear scaling

closer to the galaxy center. The shell structure appears to have a two-arm spiral-like morphology. Such a morphology of inner shells is observed in many other Type II shell galaxies (Wilkinson et al. 1987; Prieur 1990), for instance MC 0422–476 (Wilkinson et al. 2000). The minimum masking obscures the sharp-edged nature of the inner shells, which can be seen e.g. in Figure 1 in Im et al. (2017) and which distinguish them from classical spiral arms.

To constrain the shell-system age, we needed to measure the shell radii. This is ambiguous given the spiral-like morphology of the shells. Inspired by the axially symmetric shell systems (see Sect. 4), we measured the shell radii at the points where the shell edges crossed the visually determined major axis of the galaxy, as indicated in the left-hand panel of Fig. 1. A further uncertainty of the measured shell radii came from the blurriness of the shell edges. The adopted shell radii are listed in Table 1. The shells lying north (south) of the galaxy center have positive (negative) signs. The center was set to the coordinates of the brightest pixel in the central region of the galaxy ($RA = 13^{\text{h}}09^{\text{m}}47.7^{\text{s}}$, $Dec = -23^{\circ}23'0.2''$). Given the approximative character of the calculation of shell-system age (Sects. 4 and 5), the uncertainty in determining the photometric axis, the center of the galaxy, and the shell radii is probably unimportant.

3 MODEL FOR THE GRAVITATIONAL POTENTIAL

The evolution of the shell structure depends on the gravitational potential of the galaxy. We constructed the model of the gravitational potential of NGC 4993 using the measurements of the stellar component from literature and coupling them with the dark matter component via the stellar-to-halo mass relation inferred by the abundance matching technique.

The stellar component was modelled as a deprojected Sersic profile assuming a spherical symmetry. The parameters of the Sersic profile were taken from Palmese et al. (2017). We used their GALFIT output for the r -band DECam image (see Table 1 in Palmese et al. 2017): the apparent magnitude of 11.90, the effective radius of 16.74'', and the Sersic index 3.7. Similar values of the fit were derived also in Im et al. (2017). Furthermore, we assumed a constant mass-to-light ratio of 5.23 in the r -band derived by Palmese et al. (2017) from a 6dF spectrum of NGC 4993.

The mass of the dark matter halo was estimated using Equation (15) from Shankar et al. (2006) – the re-

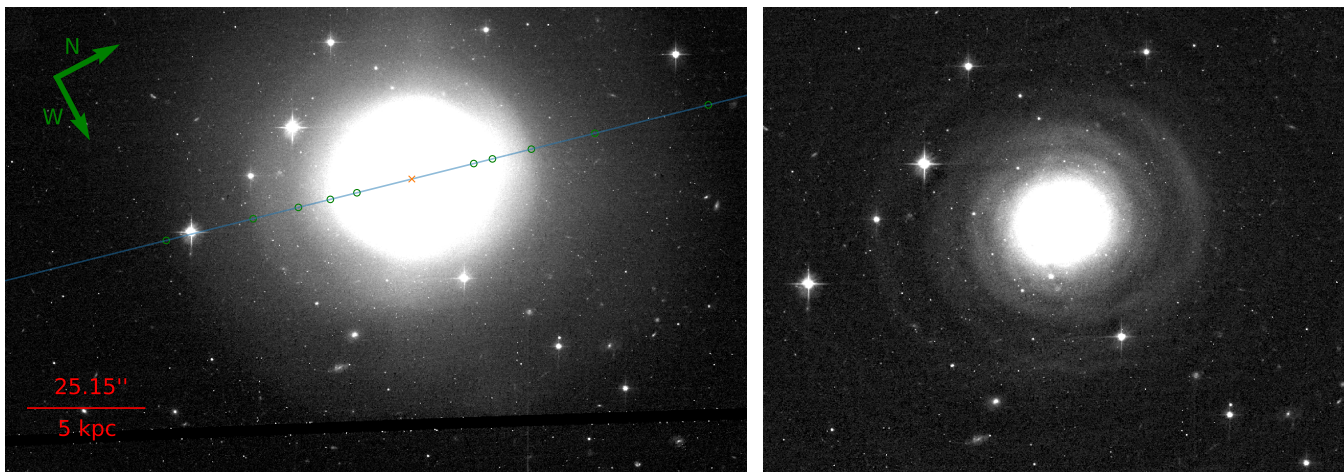


Figure 1. Image of the shell galaxy NGC 4993 (based on the HST/ACS data in the F814W filter). *Left:* The image processed by intensity scaling to show the outer shells. The blue line indicates the visually determined major photometric axis. The orange cross denotes the center of the galaxy. The green circles on the blue line mark the positions of the measurements of shell radii (Table 1). *Right:* The image processed by minimum masking technique (Bílek et al. 2016) with the filter size of 1.2'' reveals the shells close to the galaxy center. Note the two-arm spiral-like morphology of the shells.

lation between the central stellar velocity dispersion and the halo mass. The value of the central velocity dispersion, $160.0 \pm 9.1 \text{ km s}^{-1}$, was inferred from the 6dF spectrum by Palmese et al. (2017). This value is roughly consistent with the weighted mean value, $\langle \log(\sigma_0 / \text{km s}^{-1}) \rangle = 2.241 \pm 0.012$, compiled from measurements in literature by Im et al. (2017). The central velocity dispersion of 160.0 km s^{-1} corresponds to the halo mass of $M_{\text{halo}} = 193.9 \times 10^{10} M_{\odot}$. The dark matter halo was modelled by the Navarro–Frenk–White (NFW) profile (Navarro et al. 1997). The mass of the NFW halo constrains its concentration. The relation derived in Dutton & Macciò (2014) leads to the concentration parameter $c_{200} = 7.52$.

4 EVOLUTION OF SHELL RADII

Methods to compute the evolution of shell radii in a given gravitational potential analytically were developed only for axially symmetric shell systems (i.e. Type I shell galaxies, Wilkinson et al. 1987; Prieur 1990), see Quinn (1984); Dupraz & Combes (1986); Ebrova et al. (2012); Bılek et al. (2013, 2014). Type I shell systems are symmetric around the major photometric axis of the galaxy and the shells are almost circular arcs. This model assumes that the secondary galaxy was accreted on the host on a radial trajectory and that the stars released from the secondary move also on strictly radial orbits. Shells emerge on radii, where the stars are currently located near the apocenters of their orbits. Here we used Equations (1)–(3) and (12) of Ebrova et al. (2012) to calculate the time evolution of the shell radii. For more details see also Sections 9.1 and 9.2 in Ebrova (2013) or Section 2.4.1 in Bılek (2016). We note that the assumption on the radial orbits is broken to some degree for the non-axisymmetric shell system of NGC 4993. In Sect. 5, we argue that the model still gives a useful estimate of the merger time for the galaxy.

The black curves in Fig. 2 show the evolution of the

radii for the first 10 shells in the gravitational potential of NGC 4993 (stellar plus dark matter component derived in Sect. 3). The leftmost curve corresponds to the shell number one which consists of stars finishing their first orbit in the host galaxy. The shell radius increases with time and more shells emerge. Each subsequent shell is formed by stars with more finished orbital periods and thus it expands slower than the previous shell at the same radius. The older the shell system is, the more shells it possesses.

The gray regions in Fig. 2 indicate the uncertainties in the shell evolution resulting from the measurement error of the central velocity dispersion and from uncertainty of the mass-concentration relation for the NFW halo, see Sect. 3. The fastest (slowest) evolution of the shell structure is for the halo with a mass of $228.9 (162.6) \times 10^{10} M_{\odot}$ and a concentration of 9.81 (7.63). The real uncertainties of the model are probably bigger since we do not account for uncertainties of the abundance matching. Moreover, the model was not constructed to account for the shell structure with the morphology observed in NGC 4993, see Sect. 5.

The measured shell radii (Sect. 2, Table 1) are indicated as horizontal lines in Fig. 2. Red (blue) lines correspond to the shells north (south) of the center of the galaxy. Based on the position of the outermost observed shell, the merger happened at least 200 Myr ago. The overall number of the observed shells leads to the most probable time of roughly 400 Myr and estimates higher than 600 Myr being inconsistent with the model. For more details, see Sect. 5.

5 DISCUSSION

The method described in Sect. 4 was, in a more complex form, applied on a rich Type I shell system of the galaxy NGC 3923 in Bılek et al. (2013, 2014). The Type II shells are not reproduced precisely by the idealized model of a radial galactic merger with stars on radial orbits. The observed morphology of the shells in NGC 4993 indicates that the

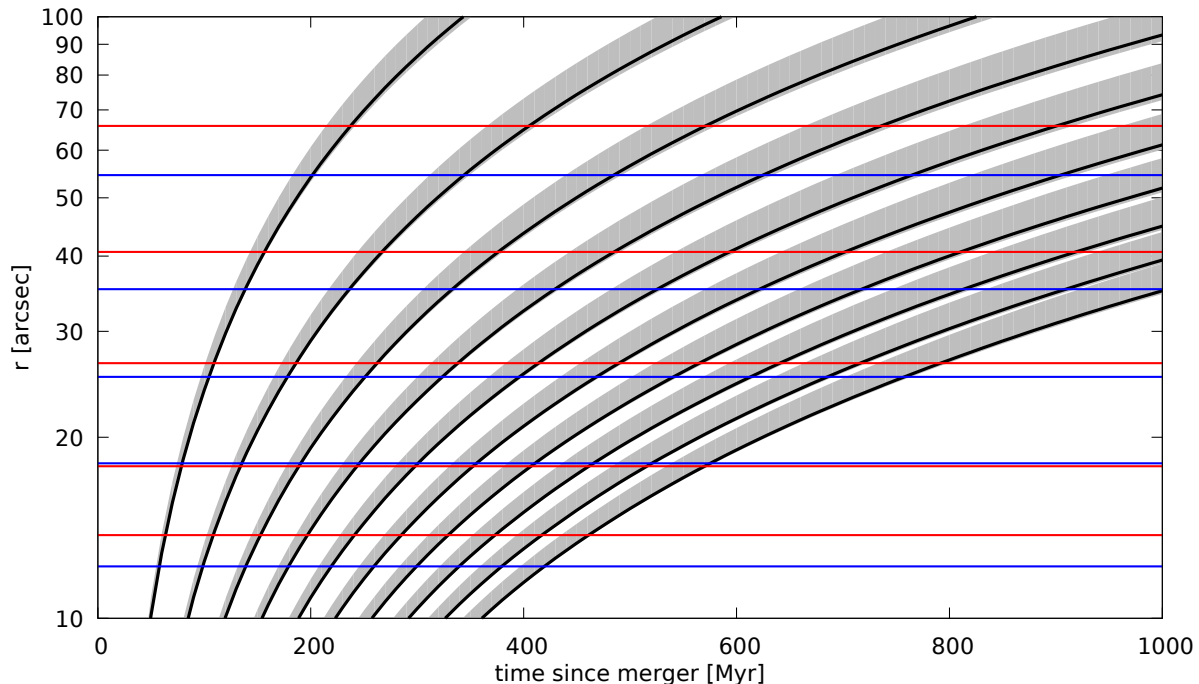


Figure 2. Black curves show the theoretical evolution of the radii for the first 10 shells in the gravitational potential of NGC 4993. Gray regions indicate uncertainties due to the halo mass and concentration. Red (blue) lines correspond to the actual shell edges north (south) of the center of NGC 4993.

galaxy accreted a smaller disk galaxy on a highly eccentric but non-radial trajectory with the disk probably inclined with respect to the orbital plane of the galactic merger, see for example Figure 3 in [Quinn \(1984\)](#) or Figure 11 in [Dupraz & Combes \(1986\)](#). It would require more detailed N -body simulations to account for such a merger and to infer the merger time with a higher accuracy.

There are two major obstacles preventing a correct reproduction of the observed distribution of shell radii by the model:

(1) The positions of the true shell edges probably lag behind the theoretical radii, since the stars on non-radial orbits have longer orbital periods for the same apocentric distances. The period of an oscillation in the radial direction is the longest for the stars on nearly circular orbits. Using the epicyclic approximation ([Binney & Tremaine 1987](#)), we derived that, in the potential of NGC 4993, the period for such particles is 1.5–1.6 times longer than for the particles on radial orbits, in the range of apocentric distances corresponding to the range of the observed shells. This means that the assumption of the radial orbits leads to the overestimation of the merger time by at most 50–60%. The actual error caused by the orbit non-radiality is probably much smaller since simulations show that the formation of shells of any type requires a highly eccentric galactic collision (e.g. [Pop et al. 2017](#)).

(2) Type II shells do not lie at one axis but each one has its midpoint at a different azimuth which cannot be determined without more detailed treating of the data and a more advanced model. Since, in NGC 4993, the radius of a shell depends on the azimuth, measuring the shell radius on the symmetry axis introduces a certain systematic error. This is probably the reason why the measured shell spacing does not

increase monotonically with the radius, in contradistinction to the model prediction.

For those reasons, in the case of NGC 4993, the model is not supposed to reproduce (at any particular time of the evolution) the observed distribution of shell radii. Nevertheless, we still can put significant constraints on the shell-system age, i.e. on the time since the merger of the galaxies, using the following knowledge: (i) The modelled evolution of the outermost shell basically corresponds the shortest possible time in which stars, released near the galactic center, could have reached the given position in the given gravitational potential of the host galaxy. This set the lower limit for the merger time. (ii) For a Type II shell system, the rate at which shells are generated is expected to be slightly slower but roughly consistent with the model. This means that at the time corresponding to the merger time, the number of observed and modelled shells, in a certain range of radii, should be comparable, even though the exact positions of the shells are not reproduced.

In the given model, the outermost detected shell of NGC 4993 cannot reach its measured radius of $66''$ (13.0 kpc) sooner than 200 Myr after the stars were stripped from the secondary galaxy. Since the individual shells of NGC 4993 are not well separated in azimuth, it is hard to infer a reliable number of the observed shells. However, the number of the predicted shell around the time 200 Myr is about half of the observed number. Thus 200 Myr can be set as a safe lower estimate of the merger time.

Around 400 Myr after the merger, the radius of the outermost observed shell corresponds to the position of the second shell in the model. At this time, also the number of the observed and predicted shells is comparable. This would

mean that the outermost observed shell is actually the shell number two. In such a situation, deeper photometric images of NGC 4993 could reveal the unobserved outer shell. Such an observation would help to improve accuracy of the inferred time of the merger of the galaxies. In case that the outer shell is not found, it can just mean that the first shell already vanished due to the lack of stars with a high-enough orbital energy.

For times around 600 Myr and higher, the model predicts too many shells too densely placed to account for the observed shells of NGC 4993. Note that only the evolution of the first ten shells is displayed in Fig. 2. However, our model of the galaxy potential does not include uncertainties of the abundance matching. If the dark matter halo of NGC 4993 is, in fact, significantly less massive than predicted by the the abundance matching, all the time estimates would shift toward higher values. Better models of the NGC 4993 gravitational potential, using for example spatially resolved spectroscopic observations, are highly desirable.

Our lower estimate of the merger time 200 Myr is in the contradiction with [Palmese et al. \(2017\)](#) claiming the merger time to be lower than 200 Myr. The estimate calculated in Section 5.1 in [Palmese et al. \(2017\)](#) is based on the assumption that the merger time is shorter than the crossing time, while the nature of the shells implies that the crossing time at the radius of the outermost shell is rather close to the merger time or lower if the first shell or shells, that were created after the merger, are not observed.

Here, we derive a broad estimate of the probability that the binary-neutron-star (BNS) progenitor of the gravitational-wave event originates in the accreted secondary galaxy. We assume that the delay-time distribution of the BNS coalescence follows t^{-1} , where t is the time since the BNS formation. We adopt a minimum delay time of 1 Myr. A typical stellar mass ratio of a shell-producing galaxy merger is around 1:10. For a 10 Gyr old stellar population in the primary galaxy and 400 Myr for the secondary, there is a roughly equal chance, that the BNS come from the old and young population. If we assume 10% of stars in secondary galaxy formed 400 Myr ago and the rest is 10 Gyr old, then the probability that the BNS originates in the secondary is about 17%.

6 SUMMARY AND CONCLUSIONS

NGC 4993 is the shell galaxy host of the GRB170817A short gamma-ray burst and the GW170817 gravitational-wave event produced during a binary neutron star coalescence. Stellar shells are known to originate in galactic merges. A scenario, in which the host galaxy recently accreted a smaller late-type galaxy, can account for the existence of the shells together with the distribution of the younger stellar population, the dust lanes in the central region, and the low-luminosity active galactic nucleus. That implies that NGC 4993 may not be the original host of the binary neutron star. The binary star could have been born in a very different environment in a galaxy with properties distinct from the properties measured for NGC 4993. Particularly, the accreted galaxy had a lower total (stellar) mass and probably a higher gas fraction with an ongoing star formation, which could had been even enhanced by the tidal

interaction prior to the galaxy disintegration. If that galaxy was indeed the original host of the binary star, then the time of the galactic merger gives an approximate lower limit of the age of the binary neutron star at the time of its coalescence.

Here we used HST/ACS image to measure the galactocentric radii of the stellar shells in the galaxy. The DECam data show additional shells neither inside nor outside the field of view of the HST image. The shell system displays a spiral-like morphology, especially in the inner parts. Abundance matching and data from literature were used to construct the model of gravitational potential of NGC 4993. We computed the evolution of the shell radii in this potential employing an analytical model of shells that consist of stars on radial orbits. We estimated the time of the galactic merger by comparing the computed and the observed shell radii.

According to the model, the galactic merger happened at least 200 Myr ago with the most probable time roughly around 400 Myr. Estimates higher than 600 Myr are improbable.

The biggest sources of the inaccuracy of the estimate are the not well-explored uncertainty of the halo mass inferred by abundance matching and the fact that the used model was developed for axisymmetric shell systems, which is not the case of NGC 4993. A better model of the gravitational potential of the galaxy and/or more detailed N -body simulations are needed for better estimates of the time of the galactic merger.

We estimate the probability that the binary-neutron-star progenitor of the gravitational-wave event originates in the accreted galaxy to be a few tens of percent.

ACKNOWLEDGEMENTS

We thank David A. Coulter and Ryan J. Foley for valuable comments and information. We acknowledge support from the Polish National Science Centre under grant 2013/10/A/ST9/00023 and 2017/26/D/ST9/00449 (IE).

Based on observations made with the NASA/ESA Hubble Space Telescope, obtained from the data archive at the Space Telescope Science Institute. STScI is operated by the Association of Universities for Research in Astronomy, Inc. under NASA contract NAS 5-26555.

This project used public archival data from the Dark Energy Survey (DES). Funding for the DES Projects has been provided by the DOE and NSF (USA), MISE (Spain), STFC (UK), HEFCE (UK), NCSA (UIUC), KICP (U. Chicago), CCAPP (Ohio State), MIFPA (Texas A&M), CNPQ, FAPERJ, FINEP (Brazil), MINECO (Spain), DFG (Germany) and the collaborating institutions in the Dark Energy Survey, which are Argonne Lab, UC Santa Cruz, University of Cambridge, CIEMAT-Madrid, University of Chicago, University College London, DES-Brazil Consortium, University of Edinburgh, ETH Zürich, Fermilab, University of Illinois, ICE (IEEC-CSIC), IFAE Barcelona, Lawrence Berkeley Lab, LMU München and the associated Excellence Cluster Universe, University of Michigan, NOAO, University of Nottingham, Ohio State University, University of Pennsylvania, University of Portsmouth, SLAC National

Lab, Stanford University, University of Sussex, and Texas A&M University.

Based in part on observations at Cerro Tololo Inter-American Observatory, National Optical Astronomy Observatory (NOAO Prop. ID: 2015A-0616, PI: H. Jerjen), which is operated by the Association of Universities for Research in Astronomy (AURA) under a cooperative agreement with the National Science Foundation.

REFERENCES

- Abbott B. P., et al., 2017, *ApJ*, **848**, L12
- Atkinson A. M., Abraham R. G., Ferguson A. M. N., 2013, *ApJ*, **765**, 28
- Bilek M., 2016, PhD thesis, PhD thesis Charles University Prague ([arXiv:1601.01240](https://arxiv.org/abs/1601.01240))
- Bilek M., Jungwiert B., Jilkova L., Ebrova I., Bartoskova K., Krizek M., 2013, *A&A*, **559**, A110
- Bilek M., Bartoskova K., Ebrova I., Jungwiert B., 2014, *A&A*, **566**, A151
- Bilek M., Cuillandre J.-C., Gwyn S., Ebrova I., Bartoskova K., Jungwiert B., Jilkova L., 2016, *A&A*, **588**, A77
- Binney J., Tremaine S., 1987, Galactic dynamics
- Cantiello M., et al., 2018, *ApJ*, **854**, L31
- Coulter D. A., et al., 2017, *Science*, **358**, 1556
- Dupraz C., Combes F., 1986, *A&A*, **166**, 53
- Dutton A. A., Maccio A. V., 2014, *MNRAS*, **441**, 3359
- Ebrova I., 2013, PhD thesis, PhD thesis Charles University Prague ([arXiv:1312.1643](https://arxiv.org/abs/1312.1643))
- Ebrova I., Jilkova L., Jungwiert B., Krizek M., Bilek M., Bartoskova K., Skalicka T., Stoklasova I., 2012, *A&A*, **545**, A33
- Fong W., et al., 2017, *ApJ*, **848**, L23
- Hernquist L., Quinn P. J., 1988, *ApJ*, **331**, 682
- Hjorth J., et al., 2017, *ApJ*, **848**, L31
- Im M., et al., 2017, *ApJ*, **849**, L16
- Levan A. J., et al., 2017, *ApJ*, **848**, L28
- Malin D. F., Carter D., 1983, *ApJ*, **274**, 534
- Navarro J. F., Frenk C. S., White S. D. M., 1997, *ApJ*, **490**, 493
- Palmese A., et al., 2017, *ApJ*, **849**, L34
- Pop A.-R., Pillepich A., Amorisco N. C., Hernquist L., 2017, preprint, ([arXiv:1706.06102](https://arxiv.org/abs/1706.06102))
- Prieur J.-L., 1990, in Wielen R., ed., Dynamics and Interactions of Galaxies. pp 72–83
- Quinn P. J., 1984, *ApJ*, **279**, 596
- Shankar F., Lapi A., Salucci P., De Zotti G., Danese L., 2006, *ApJ*, **643**, 14
- Wilkinson A., Sparks W. B., Carter D., Malin D. A., 1987, in de Zeeuw P. T., ed., IAU Symposium Vol. 127, Structure and Dynamics of Elliptical Galaxies. pp 465–466
- Wilkinson A., Prieur J.-L., Lemoine R., Carter D., Malin D., Sparks W. B., 2000, *MNRAS*, **319**, 977
- Wu Q., Feng J., Fan X., 2017, preprint, ([arXiv:1710.09590](https://arxiv.org/abs/1710.09590))

This paper has been typeset from a $\text{\TeX}/\text{\LaTeX}$ file prepared by the author.